ELSEVIER

MCN Molecular and Cellular Neuroscience

www.elsevier.com/locate/ymcne
Mol. Cell. Neurosci. 30 (2005) 149 – 157

Overexpression of drebrin A in immature neurons induces the accumulation of F-actin and PSD-95 into dendritic filopodia, and the formation of large abnormal protrusions

Toshiyuki Mizui,[a] Hideto Takahashi,[a] Yuko Sekino,[a,b,1,2] and Tomoaki Shirao[a,*,2]

[a]*Department of Neurobiology and Behavior, Gunma University Graduate School of Medicine, 3-39-22 Showa-machi, Maebashi 371-8511, Japan*
[b]*Core Research for Evolution Science and Technology, Japan Science and Technology Corporation, Kawaguchi, Japan*

Received 22 March 2005; revised 11 June 2005; accepted 30 June 2005
Available online 28 July 2005

Drebrin A is a neuron-specific F-actin binding protein, and plays a pivotal role in the spine formation. In this study, we expressed drebrin A tagged with green fluorescent protein (GFP-DA) in hippocampal neurons at 7–9 days in vitro when presynaptic terminals are not fully maturated. GFP-DA was accumulated in dendritic protrusions and formed large abnormal structures. Since these structures were similar to filopodia in terms of lack of MAP2 immunostaining, we named them "megapodia" meaning large dendritic filopodia. F-actin and PSD-95 were also accumulated in megapodia, and their amounts were significantly correlated with that of GFP-DA. However, the expression of GFP-DA did not result in the promotion of the morphological change from filopodia into spines. These results demonstrate that drebrin A accumulates spine-resident proteins via protein–protein interaction in filopodia, and suggest that the spine formation requires the concurrence of the increase of drebrin-A expression and the functional presynaptic contact.

Introduction

Dendritic spines are the postsynaptic reception regions of most excitatory synapses, and spine formation is fundamental to the development of neuronal networks (Harris, 1999; Harris and Kater, 1994; Yuste and Bonhoeffer, 2001). It has been reported that long thin protrusions from dendrites, dendritic filopodia, change into morphologically mature spines, such as mushroom or stubby spines (Dailey and Smith, 1996; Dunaevsky et al., 1999; Ziv and Smith, 1996). Previous studies suggested that the actin cytoskeleton controlled the shape of both filopodia and spines (Dunaevsky et al., 1999; Fischer et al., 1998). We have recently shown that the accumulation of spine-resident actin cytoskeleton occurs at the initial stage of the morphological change from filopodia to spines and that this accumulation is necessary for the synaptic targeting of PSD-95 (Takahashi et al., 2003). However, the molecular mechanisms that regulate the initial stage of spine formation are still unclear.

Drebrin is a major binding protein of F-actin in the brain (Asada et al., 1994; Ishikawa et al., 1994; Shirao and Obata, 1985) (for review, see Shirao, 1995; Shirao and Sekino, 2001). Drebrin inhibits the actin-binding activity of tropomyosin and α-actinin (Ishikawa et al., 1994), and suppresses actomyosin interactions (Hayashi et al., 1996). Drebrin A is a neuron-specific isoform (Kojima et al., 1993; Shirao et al., 1989; Shirao and Obata, 1986), and its expression is increased in parallel with synapse formation (Hayashi et al., 1998; Shirao et al., 1989; Shirao and Obata, 1986). In adult, drebrin A is a major drebrin isoform, and locates at dendritic spines (Hayashi et al., 1996; Shirao et al., 1987). Transfection experiments have shown that drebrin A expressed in fibroblasts remodels straight actin bundles into thick and winding bundles (Shirao et al., 1994). Overexpression of drebrin A in mature neurons resulted in the elongation of the spine length (Hayashi and Shirao, 1999). Thus, drebrin A regulates dendritic spine shapes by changing the actin cytoskeletal properties.

PSD-95 is a postsynaptic density protein that associates with receptors and cytoskeletal elements at synapses. The overexpression of PSD-95 induced the enlargement of spines, suggesting that PSD-95 regulates the spine formation (El-Husseini et al., 2000). However, we have shown that the accumulation of drebrin and F-actin in dendritic filopodia precedes that of PSD-95 during spine formation (Takahashi et al., 2003). In addition, suppression of drebrin-A expression in developing neurons attenuates not only the accumulation of drebrin and F-actin but also that of PSD-95. Furthermore, replenishment of drebrin-A expression rescues the accumulation of PSD-95. These data suggest that the increase of drebrin-A expression during neuronal development plays a pivotal

* Corresponding author. Fax: +81 27 220 8053.
E-mail address: tshirao@med.gunma-u.ac.jp (T. Shirao).
[1] Present address: Division of Neuronal Network, Inst. Med. Sci., Univ. Tokyo, Tokyo, Japan.
[2] These authors equally contributed to this work.
Available online on ScienceDirect (www.sciencedirect.com).

1044-7431/$ - see front matter © 2005 Elsevier Inc. All rights reserved.
doi:10.1016/j.mcn.2005.06.008

role in the initiation of the spine formation. If so, it would be expected that overexpression of drebrin A at an early developmental stage facilitates the accumulation of spine-resident proteins into filopodia, and promotes the formation of mature spines.

In this study, we expressed drebrin A tagged with enhanced green fluorescent protein (GFP-DA) in cultured hippocampal neurons at 7–9 days in vitro (DIV). We analyzed the effect of exogenously expressed drebrin A on the accumulation of F-actin and PSD-95, and its effect on the morphological change of dendritic filopodia.

Results

Formation of abnormal dendritic protrusions by expression of GFP-DA

To analyze morphological changes induced by drebrin A, we co-expressed GFP-DA and DsRed2 in neurons at 7–9 DIV. In these immature neurons, mature spines are seldom observed (Takahashi et al., 2003), and only trace amount of endogenous drebrin A is expressed although drebrin E, which is not neuron specific, is highly expressed (Hayashi et al., 1998; Shirao et al., 1989). Neurons co-expressing GFP-DA and DsRed2 (GD-DR neurons) formed abnormal large dendritic protrusions (arrows in Fig. 1), in which GFP-DA was highly accumulated. Similar abnormal protrusions were also observed around the cell soma (asterisks in Figs. 1A–C). DsRed2 images showed that these abnormal protrusions (arrows in Figs. 1A, E) were thick and long, and did not have a head-like structure that was a characteristic feature of the mature spine. In addition to abnormal protrusions, transfected cells also have normal filopodia (arrowheads in Fig. 1E). In comparison, control neurons expressing only DsRed2 (DR neurons) did not form any large protrusions similar to the abnormal protrusions of GD-DR neurons, although they formed normal dendritic filopodia (arrowheads in Fig. 1H).

Quantitative analyses showed that the density of dendritic protrusions of GD-DR neurons (36.9 ± 2.1 per 100 μm dendrite, n = 25 dendrites) was not different from that of DR neurons (36.0 ± 2.1 per 100 μm dendrite, n = 28 dendrites) (Fig. 2A). However, dendritic protrusions of GD-DR neurons were significantly longer and wider than those of DR neurons [the average length of dendritic protrusions of GD-DR neurons was 3.9 ± 0.1 μm (n = 600 protrusions) and that of DR neurons was 2.5 ± 0.05 μm (n = 518 protrusions); the average width of dendritic protrusions of GD-DR neurons was 1.1 ± 0.02 μm (n = 600 protrusions) and that of DR neurons was 0.7 ± 0.01 μm (n = 518 protrusions)] (Figs. 2B, C).

We classified dendritic protrusions into abnormal or normal protrusions using DsRed2 images: protrusions that were longer than 4 μm and wider than 1 μm were classified as abnormal protrusions (gray area in Figs. 2D, E); and all other dendritic protrusions were classified as normal protrusions. In GD-DR neurons, 17.5% of dendritic protrusions were abnormal protrusions. In comparison, only 0.8% of dendritic protrusions in control DR neurons were abnormal protrusions. The GFP-DA fluorescent intensity of abnormal dendritic protrusions (1336 ± 72.1 arbitrary

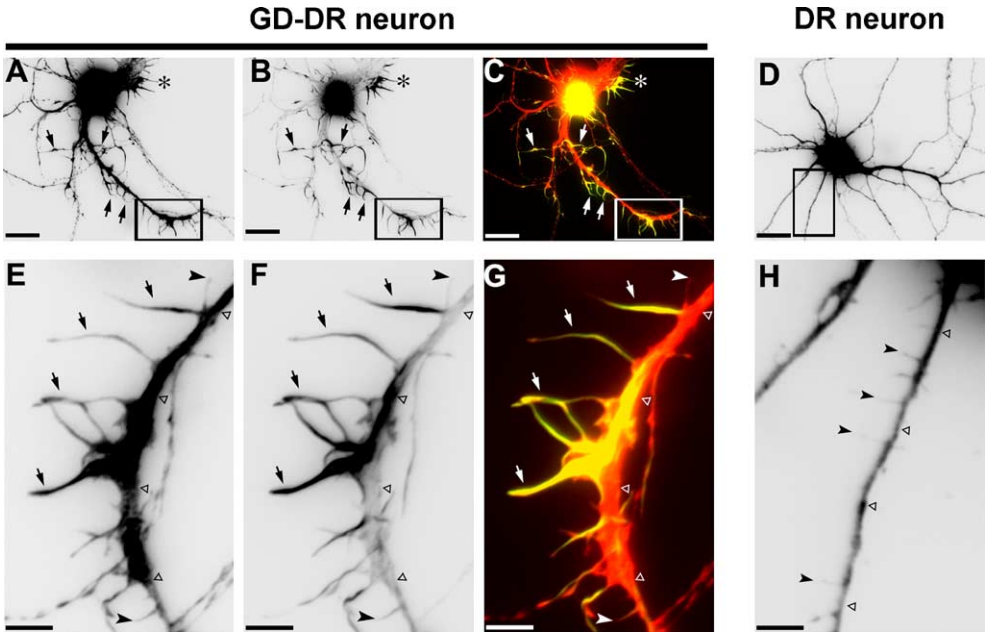

Fig. 1. Expression of GFP-DA in cultured hippocampal neurons at an early developmental stage. DsRed2 cDNA vector with GFP-DA vector or without it was microinjected into nuclei of neurons at 7 DIV, and the neurons were fixed at 9 DIV. (A–C, E–G) Neurons expressing GFP-DA and DsRed2 (GD-DR). (D and H) Control neurons expressing only DsRed2 (DR). Panels E–H are high-magnification images of the boxed region in panels A–D, respectively. Panels A, D, E, and H are DsRed2 images. Panels B and F are GFP-DA images. Panels C and G are merged images of GFP-DA (green) and DsRed2 (red) fluorescences. DsRed2 images (A and E) demonstrated that GD-DR neurons form abnormal dendritic protrusions (arrows) in addition to normal filopodia (arrowheads). Similar abnormal protrusions were also observed around the cell soma (asterisks) in panel A. Note that GFP-DA is highly accumulated in abnormal protrusions, which are observed yellow color in merged images (C and G). In control DR neurons (D and H), normal dendritic filopodia are observed (arrowheads), but no abnormal protrusions are observed. Scale bars: A–D are 20 μm; E–H are 5 μm. Open triangles indicate dendritic shafts.

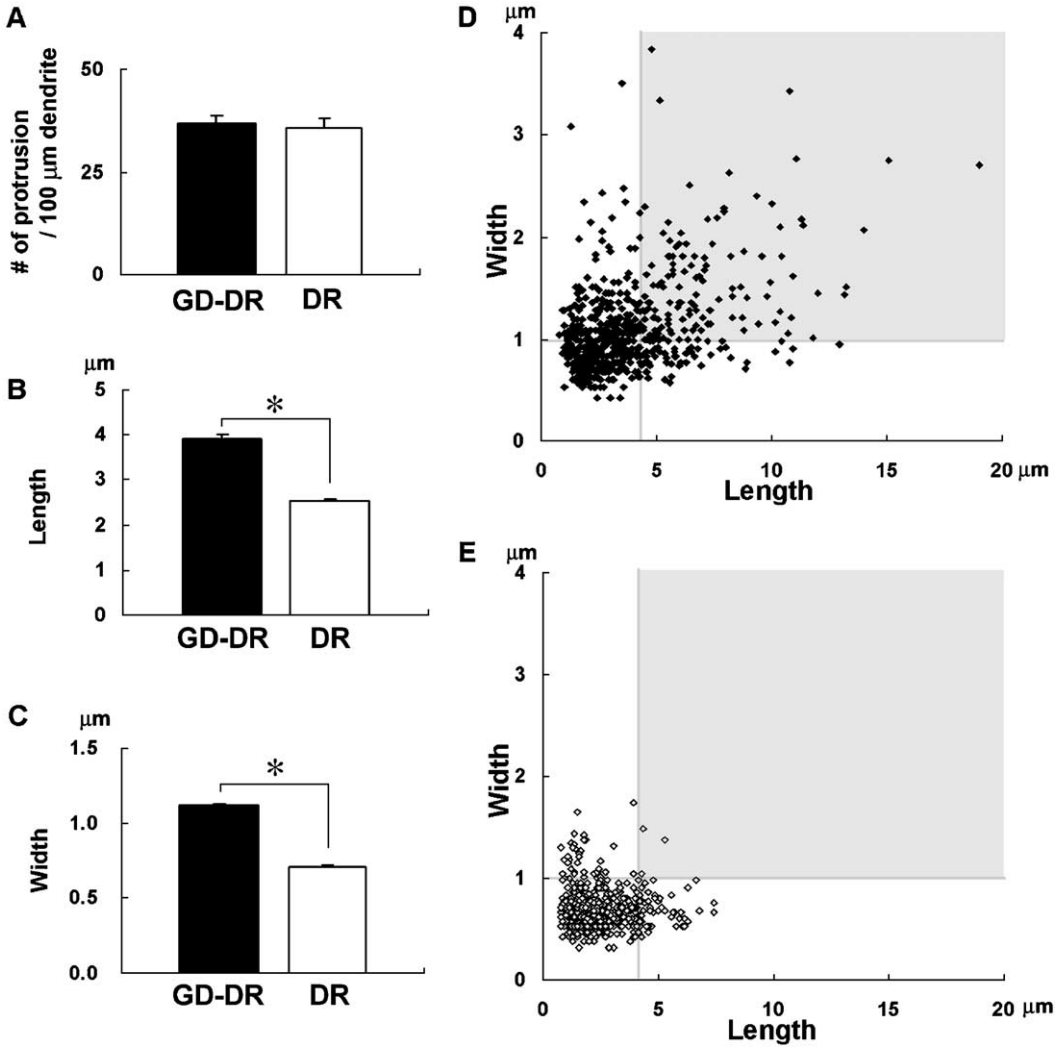

Fig. 2. Quantitative comparisons on the density, length, and width of dendritic protrusions between GD-DR neurons and control DR neurons. The density, length, and width of dendritic protrusions were manually measured using DsRed 2 images. (A) The density of dendritic protrusion of GD-DR neurons ($n = 25$ dendrites) is not different from that of control DR neurons ($n = 28$ dendrites). (B and C) The length (B) and the width (C) of dendritic protrusions of GD-DR neurons ($n = 600$ dendritic protrusions) were significantly higher than those of DR neurons ($n = 518$ dendritic protrusions) (*$P < 0.001$; t test). Histograms show means + SEM. (D and E) Scatter plots of dendritic protrusion length versus its width in GD-DR neurons (D) and in DR neurons (E). Protrusions in gray areas (length, >4 μm; width, >1 μm) are defined as abnormal.

units, $n = 141$) was significantly higher than those of normal protrusions (771 ± 48.2 arbitrary units, $n = 201$) and dendritic shafts (677 ± 78.3 arbitrary units, $n = 32$) in GD-DR neurons (Fig. 3). To analyze the effect of GFP-DA expression on the formation of abnormal dendritic protrusions in more mature neurons, which already have differentiated spines, we expressed GFP-DA in neurons at 21–23 DIV. In these more mature GFP-DA expressing neurons, only 1.3% of dendritic protrusions were abnormal protrusions.

We then analyzed effects of GFP-drebrin A expression on dendritic complexity using Sholl analysis, which quantifies the number of times the dendrites from a given neuron cross concentric circles of increasing diameter. We co-expressed GFP-DA and DsRed2 in neurons at 7–9 DIV, and immunostained them with anti-MAP2 antibody. The Sholl analyses using MAP2 immunofluorescence images showed no significant difference in dendritic complexity between DR neurons ($n = 15$ neurons) and GD-DR neurons ($n = 20$ neurons; t test) (Fig. 4).

Absence of MAP2 in the abnormal protrusions

In order to clarify whether the abnormal protrusions were similar to dendritic shafts or dendritic filopodia, we expressed GFP-DA or GFP in immature neurons, and immunostained them with anti-MAP2 antibody. In GFP-DA expressing neurons, MAP2 immunostaining was faintly observed in abnormal dendritic protrusions (arrows in Fig. 5A), in which GFP-DA was highly accumulated (arrows in Fig. 5B). Instead, intense MAP2 immunostaining was observed throughout dendritic shafts (open triangles in Fig. 5A), in which GFP-DA was observed discontinuously at the submembranous regions along dendrites (open triangles in Fig. 5B). These abnormal protrusions, in which GFP-DA was highly accumulated, were never observed upon axonal processes that did not have intense MAP2 immunostaining. The fluorescent intensity for MAP2 in the abnormal dendritic protrusions (277 ± 11.2, $n = 116$) was significantly lower than that in dendritic shafts (788 ± 81.6, $n = 28$) (Fig. 5C). In control GFP

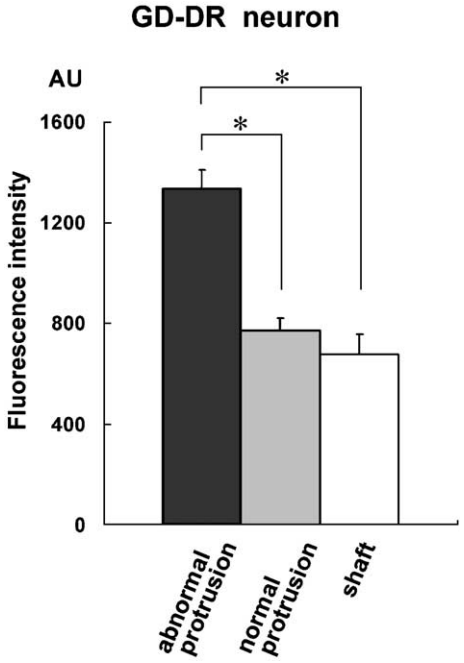

Fig. 3. Accumulation of GFP-DA in abnormal dendritic protrusions. GFP-DA and DsRed2 cDNA vectors were microinjected into nuclei of neurons at 7 DIV, and neurons were analyzed at 9 DIV. The GFP-DA fluorescent intensity of the abnormal dendritic protrusions (n = 141) was significantly higher than that of the normal protrusions (n = 201) (*P < 0.001; t test), and that of the dendritic shaft (n = 32) (*P < 0.001; t test). Histograms show means + SEM. AU, arbitrary unit.

expressing neurons, similar distribution pattern of MAP2 was observed. MAP2 immunostaining was faintly observed in dendritic protrusions and intensely observed in dendritic shafts (Figs. 5D, E). The fluorescent intensity for MAP2 in dendritic protrusions (244 ± 10.1, n = 264), which were identified by GFP images, was significantly lower than that in dendritic shafts (1020 ± 79.3, n = 15) (Fig. 5F).

Comparison of the amount of F-actin and PSD-95 between abnormal dendritic protrusions and normal dendritic filopodia

To examine whether F-actin is more highly accumulated in the abnormal protrusions than in normal dendritic filopodia, we labeled GFP-DA expressing neurons and neighboring control neurons with rhodamine-conjugated phalloidin. Dendritic filopodia in control neurons were weakly labeled (Fig. 6A), but abnormal protrusions in GFP-DA expressing neurons were intensely labeled (Figs. 6B–D). Quantitative analysis showed that RFPS (the ratio of the fluorescence intensity in dendritic protrusion to that in dendritic shaft) for F-actin of GFP-DA expressing neurons (3.58 ± 0.24, n = 208) was significantly higher than that of control neurons (0.65 ± 0.03, n = 326) (Fig. 6E).

Then, we analyzed the accumulation of PSD-95 in abnormal protrusions by immunocytochemistry. In control neurons, a faint punctate staining pattern for PSD-95 was observed mainly in dendritic shafts but seldom in dendritic filopodia (Fig. 6F). In GFP-DA expressing neurons, a similar punctate staining pattern for PSD-95 was observed in the abnormal dendritic protrusions in addition to dendritic shafts (Figs. 6G–I). Quantitative analysis showed that RFPS for PSD-95 of GFP-DA expressing neurons (1.31 ± 0.06, n = 208) was significantly higher than that of control neurons (0.45 ± 0.02, n = 113) (Fig. 6J).

Correlation of GFP-DA with F-actin and PSD-95 in the abnormal dendritic protrusions

In the abnormal dendritic protrusions, there were significant positive correlations in the fluorescent intensity between GFP-DA and F-actin (the correlation coefficient R = 0.803, n = 69) (Figs. 7A, B), and between GFP-DA and PSD-95 (R = 0.669, n = 115) (Figs. 7C, D). The linear regression analysis yielded a straight line between the intensities of GFP-DA and F-actin with an r^2 value of 0.644 and a slope of 0.87, and between those of GFP-DA and PSD-95 with an r^2 value of 0.448 and a slope of 0.14. In contrast, there was no significant correlation in the fluorescent intensity of the abnormal dendritic protrusion between GFP-DA and MAP2 (R = 0.235, n = 118) (Figs. 7E, F).

Effect of GFP-DA expression on presynaptic terminals

In order to clarify whether GFP-DA expression affects presynaptic terminals, we analyzed synapsin I clusters of control and GFP-DA expressing neurons at 7–9 DIV. In control neighboring neurons, most of synapsin I clusters were observed along dendrites (Fig. 8A). In GFP-DA expressing neurons, the distribution pattern of synapsin I clusters was similar to that in control neurons (Fig. 8B). Some, but not all, abnormal protrusions were associated with synapsin I clusters (Figs. 8C, D). Quantitative analysis demonstrated that the number of synapsin I clusters along dendrites of GFP-DA expressing neurons was not different with that of neighboring control neurons (Fig. 8E). As shown in Fig. 8F, the average area of synapsin I clusters along dendrites of GFP-DA expressing neurons (0.67 ± 0.07 μm^2, n = 6 dendrites) was similar

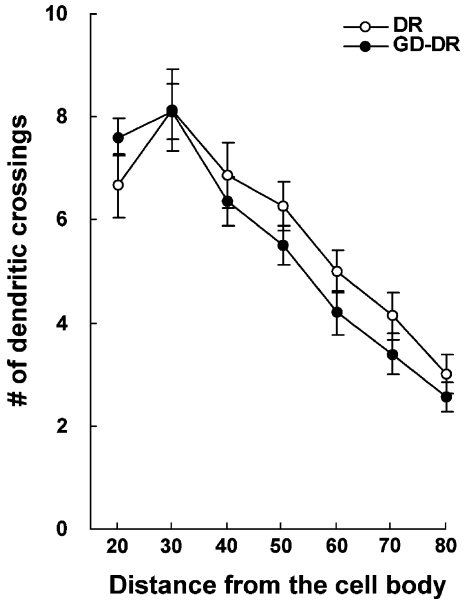

Fig. 4. Dendritic complexities of control DR neurons and GD-DR neurons. GD-DR neurons at 7–9 DIV were immunostained with anti-MAP2 antibody, and analyzed their dendritic complexity using Sholl analysis. DR neurons were used as control. The numbers of times the dendrites crossed concentric circles were not different between DR neurons (n = 15 neurons) and GD-DR neurons (n = 20 neurons; t test).

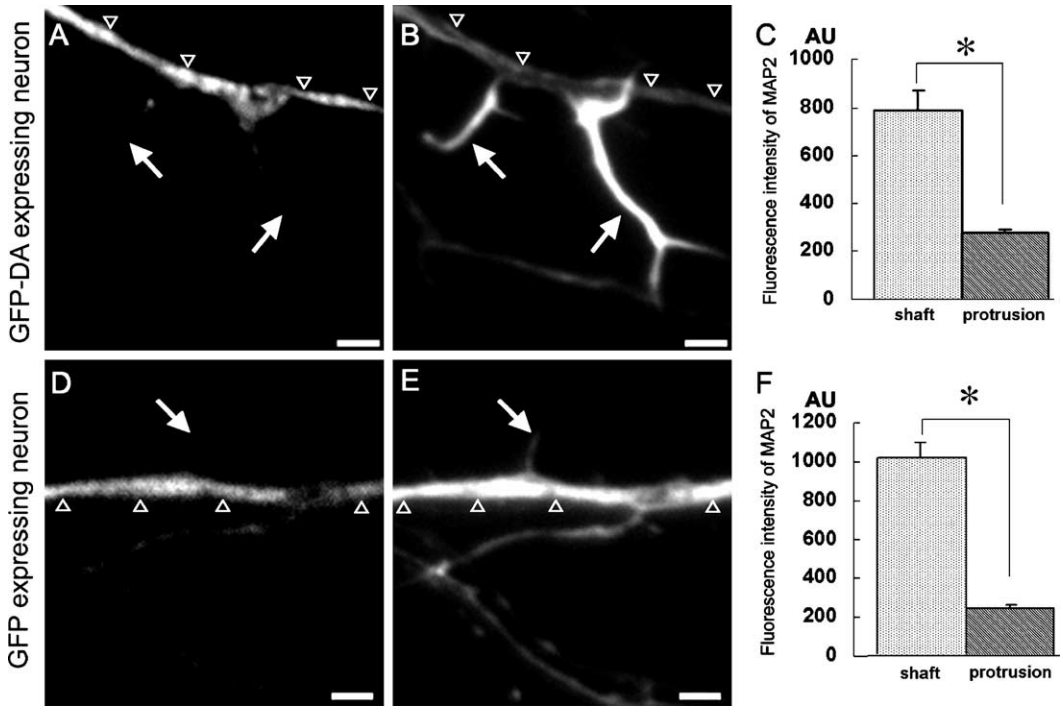

Fig. 5. Lack of MAP2 immunostaining in abnormal dendritic protrusions. GFP-DA vector was microinjected into nuclei of neurons at 7 DIV, and neurons were immunostained with anti-MAP2 antibody at 9 DIV. GFP vector was used as control. (A–C) GFP-DA expressing neuron. Fluorescence images of MAP2 (A) and GFP-DA (B) demonstrated that MAP2 was hardly observed in the dendritic protrusions in which GFP-DA is highly concentrated. Histogram (C) showed that the fluorescence intensity of MAP2 in dendritic shafts ($n = 28$) was significantly higher than that in dendritic protrusions ($n = 116$) ($^*P < 0.001$; t test). (D–F) Control neuron. Fluorescence images of MAP2 (D) and GFP (E) demonstrated that MAP2 was hardly observed in dendritic filopodia. Histogram (F) showed that the fluorescence intensity of MAP2 in dendritic shafts ($n = 15$) was significantly higher than that in dendritic filopodia ($n = 264$) ($^*P < 0.001$; t test). Arrows show dendritic protrusions. Open triangles show parent dendrites. Histograms show mean + SEM. Scale bars: 2 μm. AU, arbitrary unit.

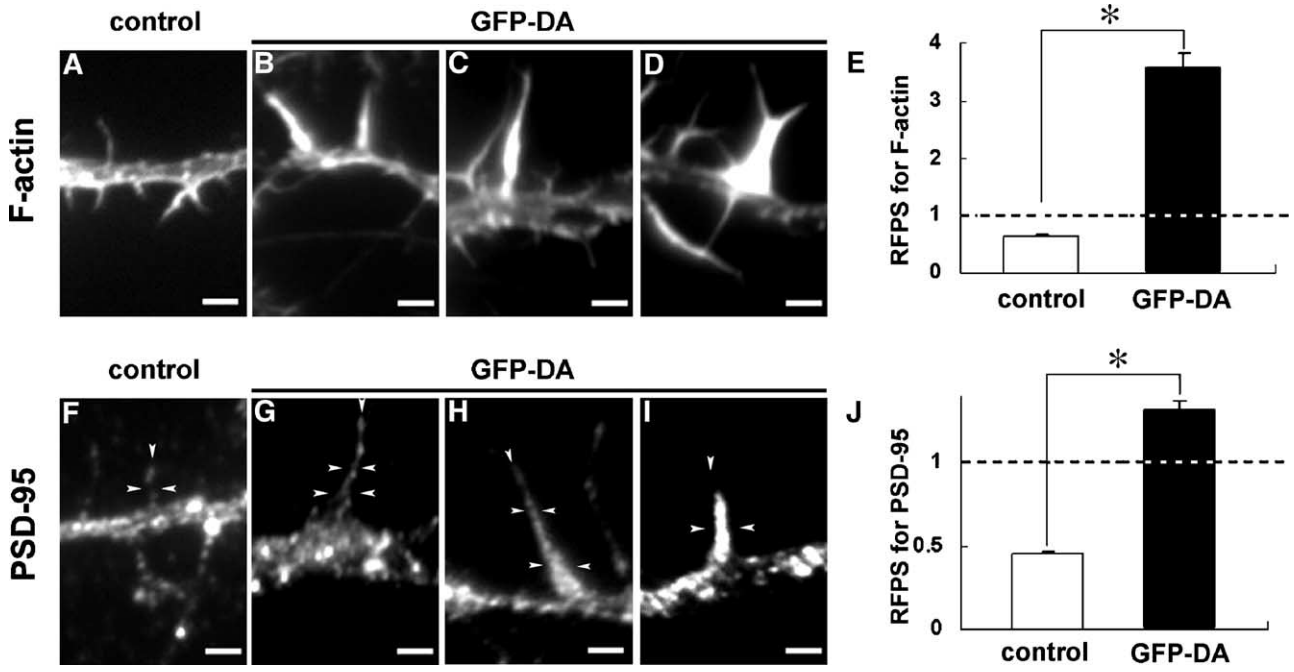

Fig. 6. Accumulation of F-actin and PSD-95 in abnormal dendritic protrusions. (A–D) Fluorescence images of F-actin in a control neighboring neuron (A) and in a neuron expressing GFP-DA (B–D). (E) Histogram showing the ratio of fluorescence intensity in dendritic protrusions to that in dendritic shafts (RFPS) for F-actin. (F–I) Fluorescence images of PSD-95 in a control neighboring neuron (F) and in a neuron expressing GFP-DA (G–I). (J) Histogram showing RFPS for PSD-95. Data showed that both RFPS for F-actin and PSD-95 of GFP-DA expressing neurons were significantly higher than those of control neurons ($^*P < 0.001$; t test). Dotted lines in panels E and J show the level that the fluorescence intensity of dendritic protrusion is equal to that of dendritic shaft. Scale bars: 2 μm. Histograms show means + SEM.

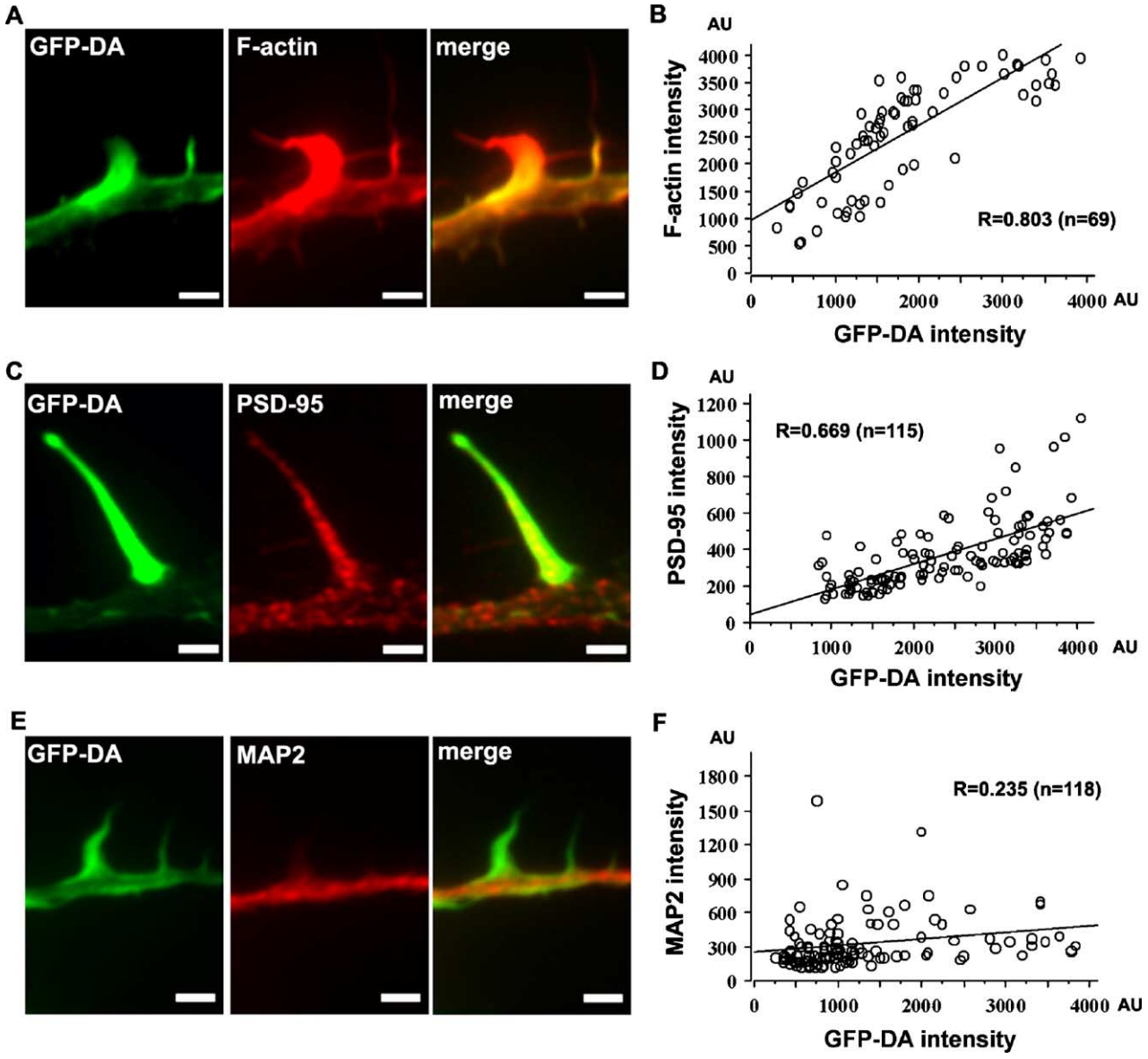

Fig. 7. Correlation of F-actin, PSD-95, and MAP2 levels with GFP-DA level. (A, C, E) Double fluorescence images of abnormal protrusions for GFP-DA and F-actin (A), for GFP-DA and PSD-95 (C), and for GFP-DA and MAP2 (E). (B, D, F) The correlations of GFP-DA and F-actin (B), of GFP-DA and PSD-95 (D), and of GFP-DA and MAP2 (F). The fluorescence intensity of GFP-DA is plotted on *x* axes (B, D, and F), and the fluorescence intensities of F-actin (B), PSD-95 (D), and MAP2 (F) are plotted on the *y* axes. There were significant positive correlations in the levels between GFP-DA and F-actin, and between GFP-DA and PSD-95. There was no significant correlation in the levels between GFP-DA and MAP2. Scale bars: 2 μm. AU, arbitrary unit.

to that of control neurons (0.68 ± 0.13 μm^2, n = 6 dendrites). Further, the average area of synapsin I clusters associated with abnormal protrusions of GFP-DA expressing neurons (0.74 ± 0.12 μm^2, n = 6 dendrites) was not significantly different from that along dendrites.

Discussion

We show here that the expression of GFP-DA in neurons at an early developmental stage results in the formation of abnormal large headless protrusions along dendrites. Expressed GFP-DA is highly accumulated in the abnormal protrusions, in which F-actin and PSD-95 are accumulated in correlation with the amount of GFP-DA. However, the expression of GFP-DA does not promote the morphological change from filopodia into spines. These results indicate that accumulation of spine-resident proteins in the filopodium is not sufficient for the spine formation.

The shape of abnormal protrusions is different from those of normal dendritic filopodia and spines. However, these abnormal protrusions are similar to dendritic filopodia in terms of the headless structure and the absence of MAP2 immunostaining. Hence, we name these abnormal protrusions “megapodia” meaning large dendritic filopodia. Sholl analysis demonstrates that the dendritic complexity of GFP-DA expressing neuron is not different from that of control neuron. This suggests that GFP-DA specifically affects megapodia formation but does not affect entire dendritic growth and arborization.

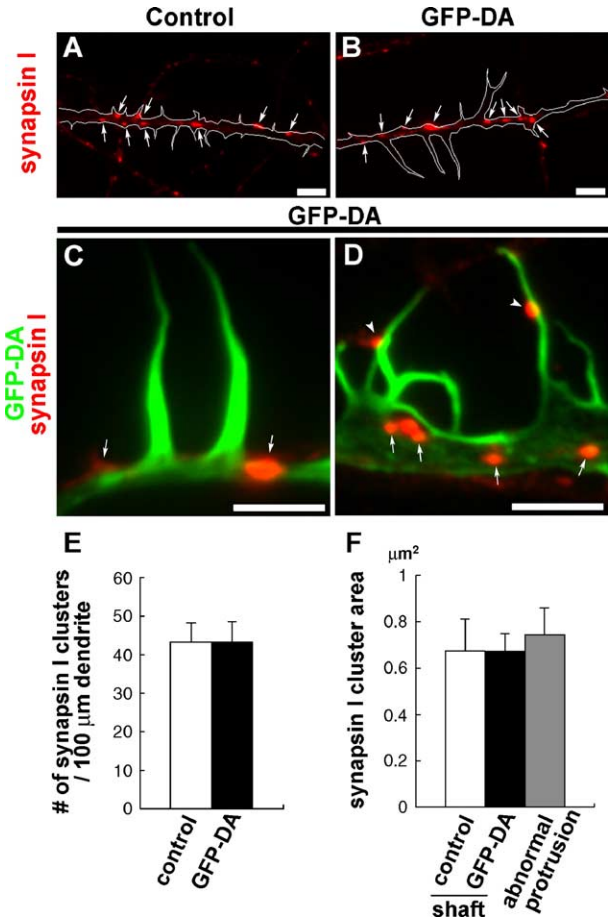

Fig. 8. Effect of GFP-DA expression on synapsin I clusters. (A and B) Low magnification of fluorescence images for synapsin I along dendrites of a control neighboring neuron (A) and of a GFP-DA expressing neuron (B). White lines indicate the contours of dendrites, which are determined with enhanced PSD-95 immunofluorescence image. (C and D) High magnification of double fluorescence images of abnormal protrusions for GFP-DA (green) and synapsin I (red) in GFP-DA expressing neurons. (E) The number of synapsin I clusters per 100-μm dendrites. There was no significant difference in the number of synapsin I clusters between control neurons (n = 12 dendrites) and GFP-DA expressing neurons (n = 12 dendrites, t test). (F) The area of synapsin I clusters. There was no significant difference in the synapsin I cluster area between control shafts (n = 6 dendrites), GFP-DA shafts (n = 6 dendrites), and abnormal protrusions (n = 6 dendrites, t test). Histograms show means + SEM. Scale bars: 5 μm.

Strong linear relationship between the amounts of F-actin and GFP-DA in megapodia indicates that drebrin A accumulates F-actin via direct protein–protein interaction. It is consistent with our previous finding that drebrin binds to actin filaments stoichiometrically in vitro (Ishikawa et al., 1994). Since the correlation coefficient R between the amounts of GFP-DA and PSD-95 is smaller than that of GFP-DA and F-actin, drebrin A probably accumulates PSD-95 via indirect protein–protein interaction. Expression of GFP-DA does not alter the density and size of synapsin I clusters along dendritic shafts. In addition, synapsin I clusters associated with megapodia are not bigger than those associated with dendritic shafts. These data indicate that upregulation of drebrin A during neuronal development in vivo directly relates to the formation of drebrin–actin complex in postsynaptic sites, and that this drebrin–actin complex enables PSD-95 to target at synapses.

Nevertheless, expression of GFP-DA in 7–9 DIV neurons does not promote the morphological maturation of filopodia into spines, and induce megapodia formation instead. In contrast, expression of GFP-DA in 21 DIV cortical neurons, which has many mature spines, results in the elongation of their spine lengths, but not in the megapodia formation (Hayashi and Shirao, 1999). Further, it has been reported that overexpression of PSD-95 in 12 DIV neurons promotes synapse maturation (El-Husseini et al., 2000).

What is the difference between our present finding and other previous findings? One possible explanation is the lack of functional presynaptic terminals at 7–9 DIV. Although it has been reported that synaptic vesicle marker proteins begin to increase in contact sites between axons and dendrites at 7 DIV, these presynaptic terminals hardly have functional synaptic vesicle turnover by 8–10 DIV (Renger et al., 2001). At 12–14 DIV, on the other hand, many functional presynaptic contacts on cultured neurons are observed (Renger et al., 2001). The lack of functional presynaptic contacts may cause megapodia formation. It is consistent to our present observation that the percentage of megapodia in total dendritic protrusions of GD-DR neurons at 21–23 DIV is less than 1/10 of that at 7–9 DIV. These indicate that spine formation requires the influence of presynaptic terminals in addition to the accumulation of drebrin A, F-actin, and PSD-95 at postsynaptic sites. However, we cannot rule out the possibility that lack of some other postsynaptic cytoskeletal molecules, such as αN-catenin, Shank, Homer, and SPAR (Abe et al., 2004; Pak et al., 2001; Sala et al., 2001), prevents spine formation.

In the elongated spines that are formed in mature neurons expressing GFP-DA, GFP-DA is highly concentrated in spine heads but not in spine necks (Hayashi and Shirao, 1999). This suggests that functional presynaptic contacts regulate the subcellular localization of drebrin A and its abundance at postsynaptic sites. When a functional presynaptic contact is absent, expressed GFP-DA may be over-accumulated through entire dendritic filopodia, and consequently dendritic filopodia may change into megapodia. Taken together, it is suggested that the spine formation requires the concurrence of the increase of drebrin-A expression and the functional presynaptic contact.

Experimental methods

Primary culture

Hippocampi were dissected from fetuses at embryonic day 18 (E18) from timed pregnant Wistar rats. Hippocampal cells were prepared by trypsinization and mechanical dissociation according to the methods described previously (Takahashi et al., 2003). Briefly, cell suspensions were plated at a density of 5000 cells/cm^2 on coverslips coated with poly-L-lysine and were incubated in Minimum Essential Medium (MEM) (Invitrogen, San Diego, CA) supplemented with 10% fetal bovine serum. After attachment of the cells, the coverslips were transferred into a culture dish containing a glial mono-layer sheet and maintained in serum-free MEM with a B27 supplement (Invitrogen). Cytosine β-D-arabinofuranoside (Sigma, St. Louis, MO) (10 μM) was added to the cultures at 4 DIV, to inhibit glial proliferation.

All animal experiments were carried out according to the Animal Care and Experimentation Committee, Gunma University,

Showa Campus (Maebashi, Japan). All efforts were made to minimize animal suffering and reduce the number of animals used.

cDNA microinjection

The construction of GFP-DA was described previously (Hayashi and Shirao, 1999). EGFP-C1 and DsRed2-C1 vectors (Clontech, Palo Alto, CA) were used as control. For transfection of these vectors into neurons, we used a microinjection method. Glass micropipettes (Femtotips; Eppendorf, Hamburg, Germany) were filled with Tris–EDTA buffer pH 8.0, which contained cDNA (0.5 μg/μl). We injected cDNA solution into nuclei of multipolar neurons at 7 DIV using a micromanipulator (Micromanipulator 5171; Eppendorf). At 2 days after the injection, the neurons were fixed and analyzed immunocytochemically.

Immunocytochemistry and fluorescent microscopy

Cells were fixed in 4% paraformaldehyde in phosphate-buffered saline pH 7.4 (PBS) at 4°C for 20 min. Fixed cells were permeabilized with 0.1% Triton X-100 in PBS for 5 min and incubated in blocking solution (3% bovine serum albumin in PBS) for 60 min. Then, the cells were incubated overnight at 4°C with a monoclonal antibody against PSD-95 (clone 7E3-1B8; Affinity BioReagents, Golden, CO), or against MAP2 (clone HM-2; Sigma). F-actin was detected with rhodamine-conjugated phalloidin (Molecular Probes, Eugene, OR). After washing with PBS for 30 min, the cells were incubated for 1 h at room temperature with secondary antibodies. Anti-mouse IgG antibodies labeled with rhodamine and with Cy5 (Chemicon, Temecula, CA) were used for detection of the monoclonal antibodies against MAP2 and against PSD-95, respectively. For analyzing Synapsin I clusters, some of neurons were further immunostained using rabbit polyclonal anti-synapsin I antibody (Chemicon) as primary antibody and anti-rabbit IgG antibodies labeled with Cy5 (Chemicon) as secondary antibody. After washing with PBS, the cells were mounted on glass slides with Perma Fluor mounting medium (Thermo Shandon, Pittsburgh, PA).

All fluorescent images of cells were obtained on a Zeiss Axioplan 2 microscope (Zeiss, Jena, Germany) equipped with a Cool Snap fx cooled CCD camera (Photometrics, Tucson, AZ), and operated with Meta Morph software (Universal Imaging, West Chester, PA) through a 63×, 1.4 numerical aperture objective lens (Zeiss). A filter set (86000 Sedat Quad; Chroma, Brattleboro, VT) was mounted in excitation and emission filter wheels (Ludl Electronic Products, Hawthorne, NY) on the microscope. All of the data were collected at 1300 × 1030 resolution at 12 bits/pixel. A single pixel in the image corresponded to a 106-nm square in the specimen plane. The images used for the comparison in this study were collected under an identical condition. Captured fluorescent images were analyzed using Meta Morph software. The signals of GFP and DsRed2 were obtained through the filters for FITC and rhodamine, respectively. We found no unsuitable fluorescent leakage of these signals through the other filters. Images for presentation were prepared using Adobe Photoshop software (Adobe Systems, San Jose, CA).

Quantification

For quantification, multipolar neurons (5–11 neurons) were selected from at least three separate cultures. The density, length, and width of dendritic protrusions were analyzed as described previously (Takahashi et al., 2003). The level of average fluorescent intensity at a dendritic protrusion or at a dendritic shaft was measured using Meta Morph software. For comparison of the amount of each protein between abnormal protrusions and normal dendritic filopodia, the ratio of the fluorescence intensity in dendritic protrusion to that in dendritic shaft (RFPS) was used.

For quantification of dendritic complexity, MAP2 immunofluorescence images of neurons were taken with 40× objective. The concentric sphere method of Sholl modified by Ma et al. (Sholl, 1953; Ma et al., 2003) was used to analyze dendritic complexity. Briefly, concentric spheres of a constant interval, 10 μm, were brought over each cell, and the cells were oriented with the center of soma as origin. Crossing of spheres were counted manually.

For quantification of the cluster number and area, clusters were defined as a staining region with a peak fluorescent level that was twofold greater than the averaged fluorescent level of dendrites. The contours of dendritic shafts were traced with enhanced immunofluorescence images. The clusters along dendritic shafts were automatically counted and measured by computer.

Statview v.5.0.1 software (SAS Institute, Cary, NC) was used for statistical analysis. Data were analyzed by unpaired Student's t test (with Welch's correction for unequal variance, if appropriate). To assess correlations between GFP-DA and other proteins, data were analyzed with Fisher's z transformation and linear regression analysis. All of the data were presented as a mean ± SEM. A P value < 0.001 was considered significant.

Acknowledgments

This work was supported by the Grants-in-Aid (12053209) for Scientific Research from the Ministry of Education, Science, Sports and Culture of Japan to TS and CREST grant to YS. The authors thank Dr. Kunihiko Obata for critical reading of the manuscript and for helpful comments. We thank Ms. Tomoko Takahashi for her excellent technical assistance.

References

Abe, K., Chisaka, O., Van Roy, F., Takeichi, M., 2004. Stability of dendritic spines and synaptic contacts is controlled by alpha *N*-catenin. Nat. Neurosci. 7, 357–363.

Asada, H., Uyemura, K., Shirao, T., 1994. Actin-binding protein, drebrin, accumulates in submembranous regions in parallel with neuronal differentiation. J. Neurosci. Res. 38, 149–159.

Dailey, M.E., Smith, S.J., 1996. The dynamics of dendritic structure in developing hippocampal slices. J. Neurosci. 16, 2983–2994.

Dunaevsky, A., Tashiro, A., Majewska, A., Mason, C., Yuste, R., 1999. Developmental regulation of spine motility in the mammalian central nervous system. Proc. Natl. Acad. Sci. U. S. A. 96, 13438–13443.

El-Husseini, A.E., Schnell, E., Chetkovich, D.M., Nicoll, R.A., Bredt, D.S., 2000. PSD-95 involvement in maturation of excitatory synapses. Science 290, 1364–1368.

Fischer, M., Kaech, S., Knutti, D., Matus, A., 1998. Rapid actin-based plasticity in dendritic spines. Neuron 20, 847–854.

Harris, K.M., 1999. Structure, development, and plasticity of dendritic spines. Curr. Opin. Neurobiol. 9, 343–348.

Harris, K.M., Kater, S.B., 1994. Dendritic spines: cellular specializations imparting both stability and flexibility to synaptic function. Annu. Rev. Neurosci. 17, 341–371.

Hayashi, K., Shirao, T., 1999. Change in the shape of dendritic spines caused by overexpression of drebrin in cultured cortical neurons. J. Neurosci. 19, 3918–3925.

Hayashi, K., Ishikawa, R., Ye, L.H., He, X.L., Takata, K., Kohama, K., Shirao, T., 1996. Modulatory role of drebrin on the cytoskeleton within dendritic spines in the rat cerebral cortex. J. Neurosci. 16, 7161–7170.

Hayashi, K., Suzuki, K., Shirao, T., 1998. Rapid conversion of drebrin isoforms during synapse formation in primary culture of cortical neurons. Dev. Brain Res. 111, 137–141.

Ishikawa, R., Hayashi, K., Shirao, T., Xue, Y., Takagi, T., Sasaki, Y., Kohama, K., 1994. Drebrin, a development-associated brain protein from rat embryo, causes the dissociation of tropomyosin from actin filaments. J. Biol. Chem. 269, 29928–29933.

Kojima, N., Shirao, T., Obata, K., 1993. Molecular cloning of a developmentally regulated brain protein, chicken drebrin A and its expression by alternative splicing of the drebrin gene. Mol. Brain Res. 19, 101–114.

Ma, X.M., Huang, J., Wang, Y., Eipper, B.A., Mains, R.E., 2003. Kalirin, a multifunctional Rho guanine nucleotide exchange factor, is necessary for maintenance of hippocampal pyramidal neuron dendrites and dendritic spines. J. Neurosci. 23, 10593–10603.

Pak, D.T., Yang, S., Rudolph-Correia, S., Kim, E., Sheng, M., 2001. Regulation of dendritic spine morphology by SPAR, a PSD-95-associated RapGAP. Neuron 31, 289–303.

Renger, J.J., Egles, C., Liu, G., 2001. A developmental switch in neurotransmitter flux enhances synaptic efficacy by affecting AMPA receptor activation. Neuron 29, 469–484.

Sala, C., Piech, V., Wilson, N.R., Passafaro, M., Liu, G., Sheng, M., 2001. Regulation of dendritic spine morphology and synaptic function by Shank and Homer. Neuron 31, 115–130.

Shirao, T., 1995. The roles of microfilament-associated proteins, drebrins, in brain morphogenesis: a review. J. Biochem. (Tokyo) 117, 231–236.

Shirao, T., Obata, K., 1985. Two acidic proteins associated with brain development in chick embryo. J. Neurochem. 44, 1210–1216.

Shirao, T., Obata, K., 1986. Immunochemical homology of 3 developmentally regulated brain proteins and their developmental change in neuronal distribution. Brain Res. 394, 233–244.

Shirao, T., Sekino, Y., 2001. Clustering and anchoring mechanisms of molecular constituents of postsynaptic scaffolds in dendritic spines. Neurosci. Res. 40, 1–7.

Shirao, T., Inoue, H.K., Kano, Y., Obata, K., 1987. Localization of a developmentally regulated neuron-specific protein S54 in dendrites as revealed by immunoelectron microscopy. Brain Res. 413, 374–378.

Shirao, T., Kojima, N., Nabeta, K., Obata, K., 1989. Two isoforms of drebrins, developmentally regulated brain protein, in rat. Proc. Jpn. Acad. 65, 169–172.

Shirao, T., Hayashi, K., Ishikawa, R., Isa, K., Asada, H., Ikeda, K., Uyemura, K., 1994. Formation of thick, curving bundles of actin by drebrin A expressed in fibroblasts. Exp. Cell Res. 215, 145–153.

Sholl, D.A., 1953. Dendritic organization in the neurons of the visual and motor cortices of the cat. J. Anat. 87, 387–406.

Takahashi, H., Sekino, Y., Tanaka, S., Mizui, T., Kishi, S., Shirao, T., 2003. Drebrin-dependent actin clustering in dendritic filopodia governs synaptic targeting of postsynaptic density-95 and dendritic spine morphogenesis. J. Neurosci. 23, 6586–6595.

Yuste, R., Bonhoeffer, T., 2001. Morphological changes in dendritic spines associated with long-term synaptic plasticity. Annu. Rev. Neurosci. 24, 1071–1089.

Ziv, N.E., Smith, S.J., 1996. Evidence for a role of dendritic filopodia in synaptogenesis and spine formation. Neuron 17, 91–102.